

Structure of the *A* Band in Thallium-Doped KCl and Its Temperature Dependence

A. A. Braner and A. Halperin

*Physics Department, The Hebrew University of Jerusalem, Jerusalem, Israel*

(Received 3 June 1970)

The *A* band in KCl:Tl has been resolved into its components using a computer. The observed absorption band is fitted quite accurately by the sum of two Gaussians ( $A_1$  and  $A_2$ ) throughout the temperature range 4–700 °K. Absorption cross sections ( $\sigma_{01}, \sigma_{02}$ ), half-widths ( $H_1, H_2$ ), peak positions ( $E_{01}, E_{02}$ ) for  $A_1$  and  $A_2$ , and their separation ( $\Delta E$ ) are given as functions of temperature. The parameters were found to be independent of the Tl concentration. The area under the *A* band decreased smoothly by about 10% on warming from 4 to 700 °K, while the areas under  $A_1$  and  $A_2$  reached a maximum and minimum, respectively, near 160 °K. At 4 °K, the peak positions were  $E_{01} = 5.014$  eV (2473 Å),  $E_{02} = 5.062$  eV (2449 Å) and the half-widths were  $H_1 = 0.060$  and  $H_2 = 0.067$  eV. On warming,  $H_1$  increases as  $[\coth(\theta/T)]^{1/2}$  with  $\theta_1 = 27$  °K.  $H_2$  remains constant up to about 160 °K. At higher temperatures, it can be approximated by the above law with  $\theta_2 = 100$  °K.  $\Delta E$  follows the same law with  $\theta_3 = 100$  °K. This behavior supports the theory in which the structure is due to the dynamical Jahn-Teller effect.

## I. INTRODUCTION

The optical absorption of alkali-halide crystals containing heavy-metal ions (such as thallium) has been widely studied.<sup>1–6</sup> Three absorption bands (*A*, *B*, and *C*) in the ultraviolet are attributed to transitions between molecular orbitals of the type  $(a_{1g})^2 - (a_{1g})(t_{1u})$ . The *A* band is assigned to the spin-forbidden transition  $^1A_{1g} - ^3T_{1u}$  (equivalent to  $^1S_0 - ^3P_1$  in the free thallos ion). In early theoretical calculations<sup>7,8</sup> these bands were expected to be Gaussian in shape. Accurate measurements, however, revealed a structure in the bands. For the *A* band in KCl:Tl, the structure was less evident at low temperatures, when it appeared symmetrical. But at higher temperatures the band turned highly asymmetric, pointing to complexity in its structure.<sup>3,4</sup> The exact structure of the *A* band is still unclear. Most investigators just stated that it has a doublet structure; others claimed a triplet structure.<sup>3,5,6</sup> One of the later investigators<sup>3</sup> described the *A* band in KCl:Tl at 571 °K as composed of three Gaussian components. Recently Esser and Levy<sup>6</sup> used a computer to analyze the absorption bands of KCl:Tl. They found the *A* band to be composed of two Gaussian components at low temperatures (up to nearly 200 °K) and of three components at higher temperatures. Their measurements were limited to the temperature range of 20–299 °K.

In the present work, the structure of the *A* band in KCl:Tl has been studied in detail over the temperature range 4–700 °K. Two Gaussians were found to describe quite accurately the *A* band throughout the whole temperature range under examination.

## II. EXPERIMENTAL

Single crystals of KCl containing thallium at various concentrations were grown by the Bridgman method in vacuum. High-purity KCl powder in a quartz tube was heated to 500 °C under continuous pumping and flushed several times with pure argon during the process to remove water vapor, adsorbed oxygen, and other volatile compounds. Thallium chloride was then added; the mixture was flushed again with argon and was pumped at 150 °C. Finally, the tube was sealed off and put into a furnace with a suitable temperature gradient for crystallization. The crystal was then cooled to room temperature over a 30-h period. Plates (8 × 11 mm) were cleaved from the ingot, and polished to obtain a high transparency and the desired thickness. In most cases the thickness was chosen to give an optical density of less than 2 at the peak of the *A* band. Actual thickness varied from less than 0.4 mm for the high Tl concentrations, up to 6 mm or more for the low concentrations.

Part of the thallium escaped during the process of preparation and crystallization, and concentrations in the samples were some 10–20% of those in the starting material. The actual concentration was determined from the *A* band absorption using the formula given by Wagner,<sup>5</sup>

$$C = 1.062 \times 10^{-6} \mu_A^{\max}, \quad (1)$$

where  $C$  is the molar fraction of thallium in the sample, and  $\mu_A^{\max}$  is the absorption coefficient in  $\text{cm}^{-1}$  at the maximum of the *A* band at 293 °K. This formula seems to agree within a few percent with Tl concentrations determined by Delbecq *et al.* using neutron-activation analysis.<sup>9</sup>

TABLE I. Thickness  $d$  and concentration of thallium  $C$  for samples examined.

Sample No.	$d$ (cm)	$10^6 C$ (mole/mole)
53	0.222	10
55	0.275	6.5
68	0.055	36
81	0.084	23
91	0.626	1.7

Crystals were mounted in a metal vacuum cryostat provided with quartz windows, a thermocouple, and a heating element. It enabled optical measurements from liquid-helium temperature up to above 700°K. The crystal was imbedded in a copper holder and pressed with a copper cover plate to the main block by screws, leaving only openings for optical measurements. To eliminate possible effects of strain in the crystal, the cover was left somewhat loose in some experiments and thermal contact from the holder to the crystal was ensured by surrounding the crystal with indium. Heating to above 150°C caused the indium to melt and adhere to both the copper holder and the edges of the crystal, making good thermal contact. No significant differences were observed in the temperature dependence of the  $A$  band as measured using the two methods of mounting of the crystals.

Absorption measurements were carried out with a Cary 14 spectrophotometer, for which purpose the sample compartment of the Cary was adapted to accommodate the cryostat. Slow scanning rates of the spectrum were chosen in order to eliminate effects due to the relatively slow response of the chart recorder (more than 1 sec for full scale deflection). This was especially important with the comparatively narrow bands at low temperatures.

Some spectra were taken at a scanning rate as low as 0.5 Å per second. Spectral slit widths were less than 3 Å in all measurements. Wavelengths were calibrated using the 2536-Å mercury line, and repeatedly checked, ensuring an accuracy of better than 1 Å (2 meV) in the measurements.

When the optical density at the maximum of the  $A$  band was about 2 or higher, it was found necessary to eliminate effects of the emission on the measured optical density. For this purpose, two quartz cells (2-cm optical path) filled with chlorine were inserted into the reference and sample beams of the Cary. The cell in the sample beam was put between the cryostat and the detector, absorbing almost completely the emission near 3000 Å. Insertion of the chlorine filters introduced a small change in the zero line of the spectrophotometer, which was properly corrected.

### III. COMPUTATIONS

Measured optical densities (at intervals of 2–5 Å) were analyzed by a computer (CDC 6400). Resolving a compound band into its components involves a least-squares fit, in which the set of component bands whose sum gives the smallest deviation from the measured band is chosen. Out of several nonlinear least-squares computer programs attempted,<sup>10</sup> we chose the BMDX85 program,<sup>10</sup> which gave the same results as the others, but was more convenient to use.

Experimental results (see below) suggested that the  $A$  band is composed of Gaussian components. The problem was to find the number of components involved. Each absorption curve was, therefore, twice analyzed resolving it into two Gaussians (allowing six free parameters), and then into three Gaussians (nine parameters). Mean errors were quite small in both the two- and three-Gaussian fits. Another check was, therefore, made to help to decide between the two analyses: The program

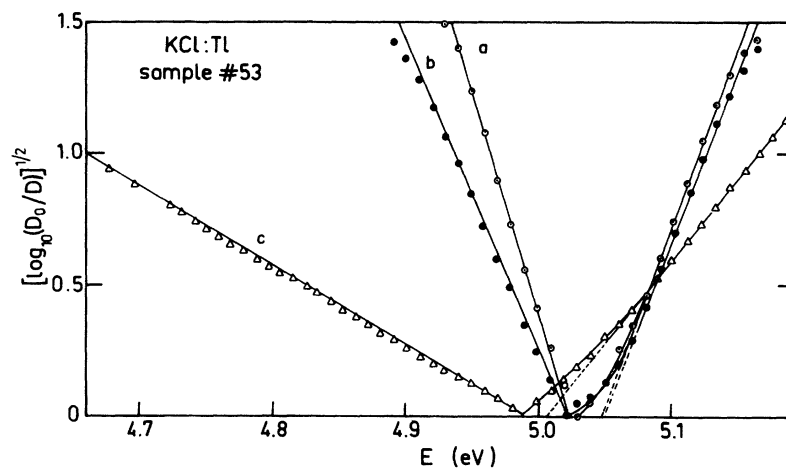


FIG. 1.  $A$  band in KCl:Tl plotted as  $[\log_{10}(D_0/D)]^{1/2}$  vs the energy  $E$ . Curves  $a$ ,  $b$ , and  $c$  at 4, 80, and 611°K, respectively.

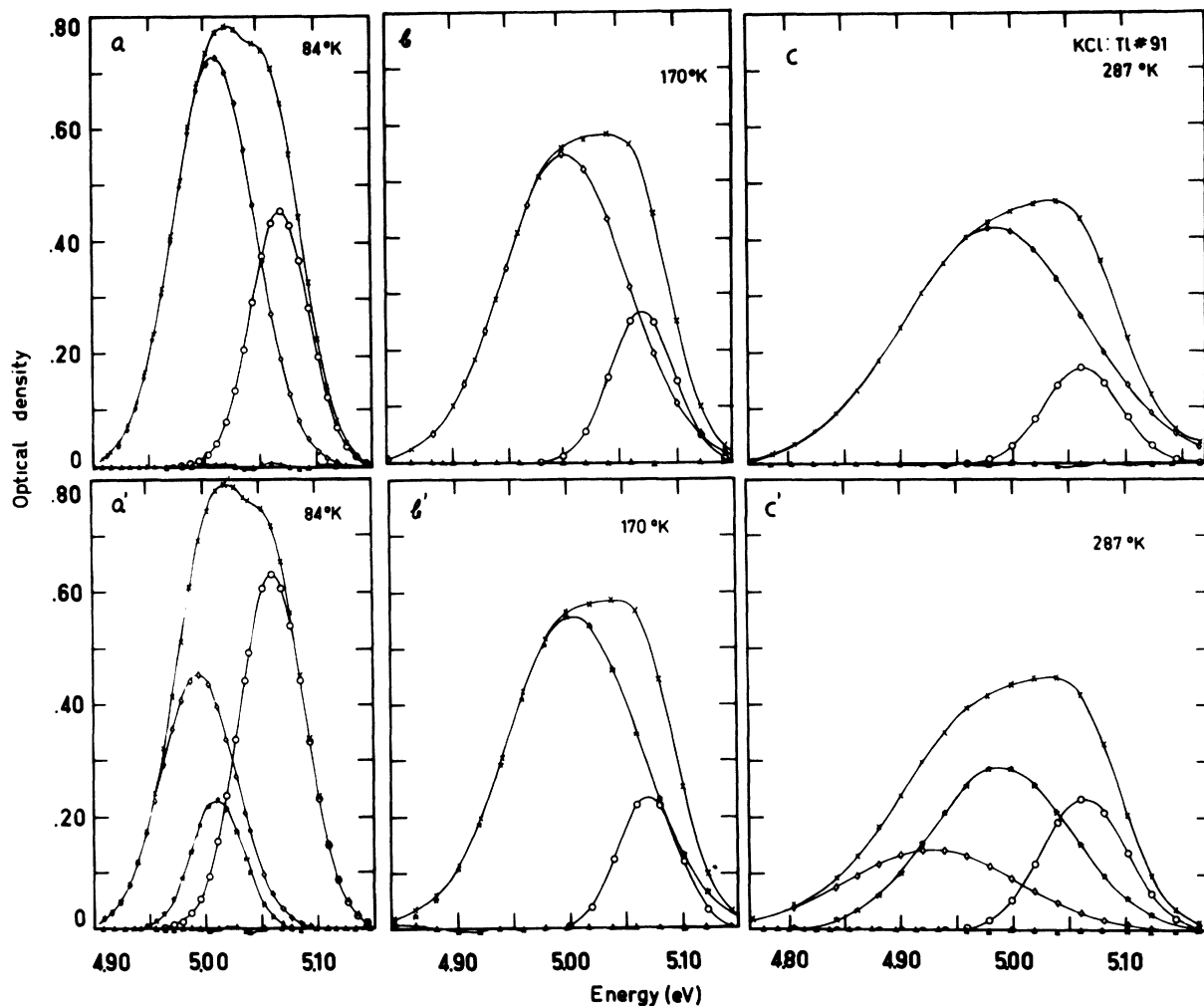


FIG. 2. Resolution of the A band of sample 91 into two Gaussians (upper curves), and three Gaussians (lower curves). Curves *a*, *a'*; *b*, *b'*; and *c*, *c'* at 84; 170; and 287 °K, respectively.  $\times$ , observed A band (corrected);  $\diamond$ , low-energy component; O, high-energy component;  $\Delta$ , error curve; and  $\star$ , third component (in lower curves). For the sake of clarity, the figure shows only one out of two or three measured points.

has been divided into two steps, computing first just one Gaussian, fitting the low-energy tail of the observed A band. This "low-energy component" was then subtracted from the observed A band, and the second Gaussian was computed by best-fitting the difference.

Measured optical densities had to be corrected for reflection losses and for some scattering at the crystal faces. In a few cases this was done by drawing a "zero line," and subtracting accordingly. It proved, however, more accurate and more convenient to let the computer make these corrections. This was done by adding to the function to be computed an expression with two more parameters:  $aE^4 + b$ , where  $E$  is the energy,  $a$  is a parameter allowing for the scattering,<sup>11</sup> and  $b$  is the zero-line parameter.

#### IV. RESULTS

Five of the crystals under examination were investigated in detail. Thicknesses and thallium concentrations in these samples are given in Table I. Other crystals examined, containing higher or somewhat lower concentrations of thallium, exhibited essentially the same behavior. The analysis of their absorption curves, however, was less accurate because the optical densities were either too high or too low.

##### A. Shape of A Band and Its Relation to Gaussian Curves

A single Gaussian absorption band is described by

$$D(E) = D_0 \exp\left[-(4 \ln 2/H^2)(E_0 - E)^2\right], \quad (2)$$

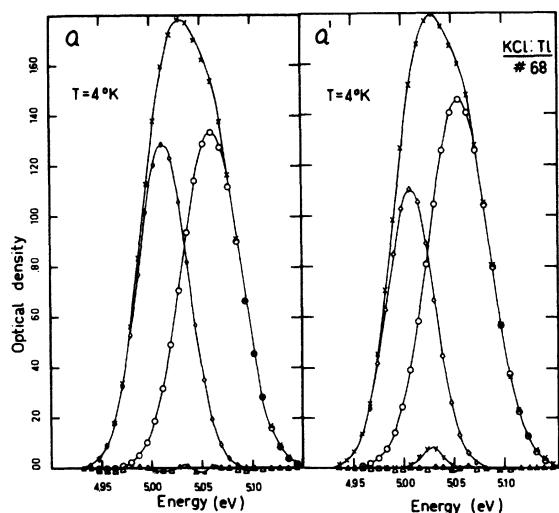


FIG. 3. Same as Fig. 2 but for sample 68 at 4°K.

where  $D$  is the optical density at the energy  $E$ ,  $D_0$  is the peak density,  $E_0$  is the energy at the peak, and  $H$  is the half-width of the band.

A convenient check of the deviation of observed absorption curves from Gaussian bands can be obtained from plots of  $[\log_{10}(D_0/D)]^{1/2}$  vs  $E$ . Figure 1 gives such plots for the absorption of sample 53 at 4, 80, and 611°K (curves  $a$ ,  $b$ , and  $c$ , respectively). Deviations from the  $V$ -shaped curves expected from Eq. (2) for a pure Gaussian are evident. Still, the observed bands are related to Gaussian curves as indicated by the wings following straight lines over a wide range, as expected for a combination of partly overlapping Gaussians. The better fit to a straight line of the low-energy wing indicates that this tail is almost purely Gaussian, practically unaffected by the overlap.

In spite of the overlap, one can get from the slopes in Fig. 1 approximate half-widths. Thus, the low-energy sides of curves  $a$ ,  $b$ , and  $c$  give half-widths of 0.065, 0.080, and 0.37 eV, respectively, and their high-energy wings give values of 0.080, 0.084, and 0.178 eV, respectively.<sup>12</sup> One also notices that half-widths of the high-energy component remain almost constant at low temperatures.

#### B. Resolution of A Band

A few examples of the computed Gaussians obtained by resolving the A band into two and three Gaussians, respectively, are shown in the upper and lower halves of Fig. 2. The curves in Fig. 2 were obtained for sample 91. Curves  $a$ ,  $a'$  were taken at 84°K,  $b$ ,  $b'$  at 170°K, and  $c$ ,  $c'$  at 287°K. The figures show the observed A band (corrected for zero line and scattering), the Gaussian compo-

nents, and the error curves (differences between the A band and the sum of the components at each energy). In Fig. 2, curve  $b'$  shows just two Gaussians (with the third negligibly small). Such failures in resolution into three components occurred occasionally also at other temperatures, revealing one of the weaknesses of the three-Gaussian resolution (see below). Figure 3 shows the two-Gaussian resolution (curve  $a$ ), and the three-Gaussian one (curve  $a'$ ) for sample 68 at 4°K.

Mean errors for sample 91 throughout the temperature range of 4–530°K are shown in Fig. 4. The errors are quite small and can be accounted for by the errors in recording and reading the optical densities. The three-Gaussian resolution (curve  $b$ ) is seen to give somewhat smaller errors compared to those obtained by the two-Gaussian resolution (curve  $a$ ). The shape of the mean-error-vs-temperature curves was nearly the same for all samples; namely, the errors were comparatively high at very low temperatures, reached a minimum near 170°K, then increased to a small maximum at about 400°K, after which they decreased again.

In spite of the smaller errors, the three-Gaussian analysis proved not to be reliable; the resolution depended strongly on the initial guesses of the parameters given to the computer, and the curves describing the dependence of the parameters on temperature showed irregularities. With two Gaussians, on the other hand, the resolution was independent of the initial guesses, and the temperature dependence of the parameters gave smooth curves (see Figs. 6–10).

The analysis of the bands was now repeated using the two-step method (see Sec. III). Two examples are shown in Fig. 5. In Fig. 5(a) (sample 55, 117°K), the low-energy Gaussian ( $A_1$ ) was computed from experimental points with energies up to 4.97 eV. The figure also shows the difference curve and the Gaussian best-fitted to it ( $A_2$ ). Figure 5(b) gives similar results obtained from the A band of sample 55 at 552°K. This time, only points up to 4.83 eV were used for the computation of  $A_1$ . Similar results were obtained by this method

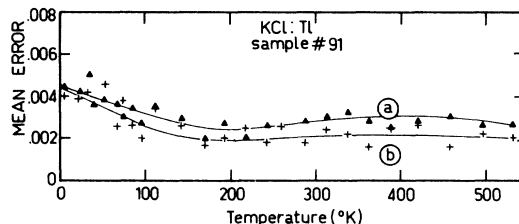


FIG. 4. Mean errors (in density units) obtained in the resolutions of sample 91. Curve  $a$ , two-Gaussian resolution; curve  $b$ , three-Gaussian resolution.

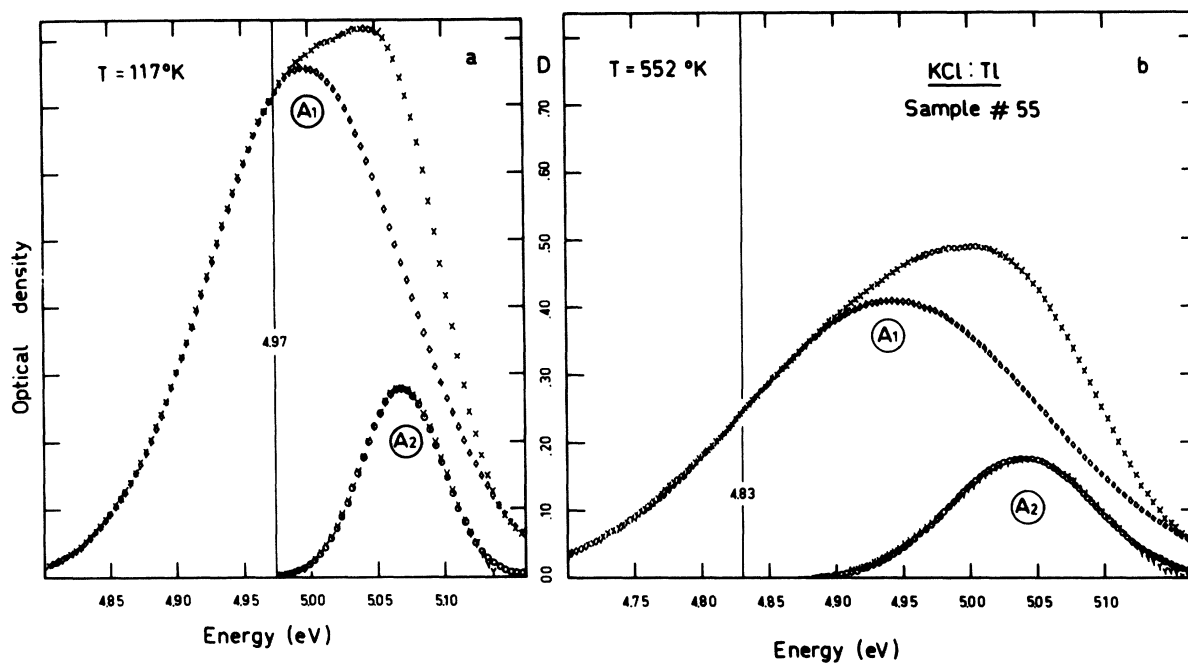


FIG. 5. Two-step analysis of the A band:  $A_1$ , low-energy Gaussian ( $\diamond$ ) computed from points up to the indicated limits.  $A_2$ , high-energy Gaussian ( $\circ$ ) computed from the difference curve ( $\gamma$ ): a, at 117°K; b, at 552°K.

at all temperatures above about 80°K. At lower temperatures, and especially near liquid-helium temperature, the strong overlap of the components did not leave enough of a pure Gaussian tail at the low-energy end for the calculation of  $A_1$ . The good fit of the difference curve to just one Gaussian ( $A_2$ ) supports strongly the two-component analysis of the A band. The accuracy of the resolution, however, can be expected to be better using the one-

step two-Gaussian resolution, which was used in all the curves shown below.

### C. Parameters of Gaussian Components and Their Temperature Dependence

A Gaussian curve [Eq. (2)] is fully characterized by three parameters, namely,  $D_0$ ,  $E_0$ , and  $H$ . In the following we use the subscript 1 for the parameters of  $A_1$  and 2 for those of  $A_2$ . The average half-widths

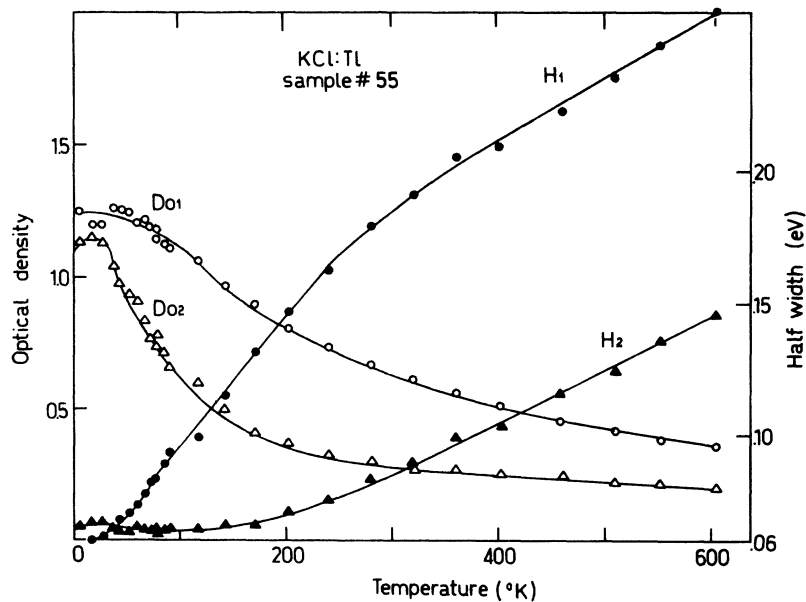


FIG. 6. Temperature dependence of the peak densities ( $D_{01}$  and  $D_{02}$ ) and of the half-widths ( $H_1$  and  $H_2$ ) of  $A_1$  and  $A_2$  for sample 55.

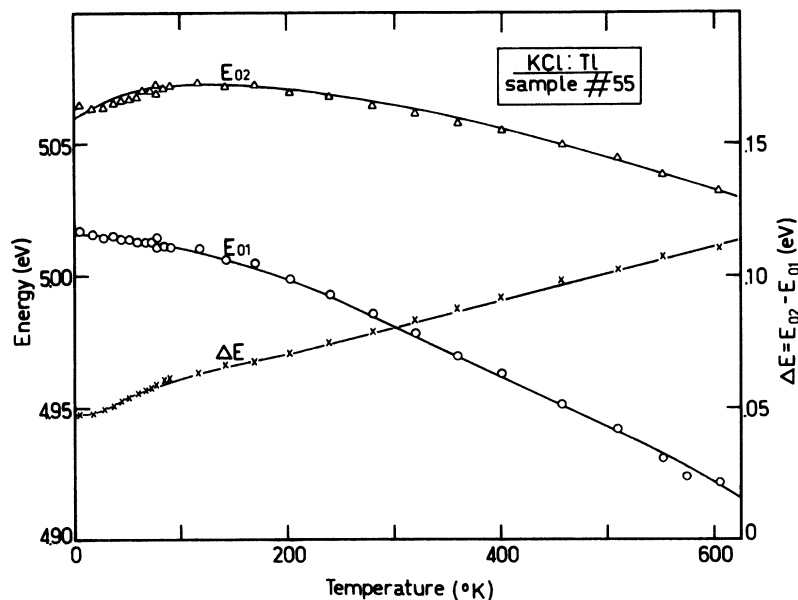


FIG. 7. Temperature dependence of the energies of the maxima ( $E_{01}$  and  $E_{02}$ ), and the separation ( $\Delta E$ ) of  $A_1$  and  $A_2$ .

at liquid-helium temperature were  $H_1 = 0.060$  and  $H_2 = 0.067$  eV, and the average peak energies at the same temperature were  $E_{01} = 5.014$  and  $E_{02} = 5.062$  eV.

Further information on the nature of the bands can be obtained from the dependence on temperature of the parameters. Figure 6 gives the temperature dependence of  $D_{01}$ ,  $D_{02}$  and  $H_1$ ,  $H_2$  of sample 55 over the range 4–605 °K.  $D_{01}$  falls moderately with temperature over the whole range.  $D_{02}$ , on the other hand, falls sharply on heating to about 150 °K, and decreases much slower at higher temperatures. The temperature dependence of the half-widths is also different for the two components.  $H_1$  starts to

increase at about 25 °K and has a value of about 0.26 eV at 600 °K, while  $H_2$  remains almost constant up to about 150 °K and increases noticeably only at higher temperatures.

Figure 7 describes the temperature dependence of  $E_{01}$  and  $E_{02}$ , and of the separation  $\Delta E = E_{02} - E_{01}$ , again for sample 55.  $E_{01}$  falls very slowly up to nearly 150 °K, and faster on further heating.  $E_{02}$  increases slightly on warming to about 100 °K, and only then shifts to lower energies. The separation increases from 0.047 eV at 4 °K to 0.11 eV at 600 °K.

The product  $HD_0$  for a Gaussian band is proportional to the area under the curve and, therefore,

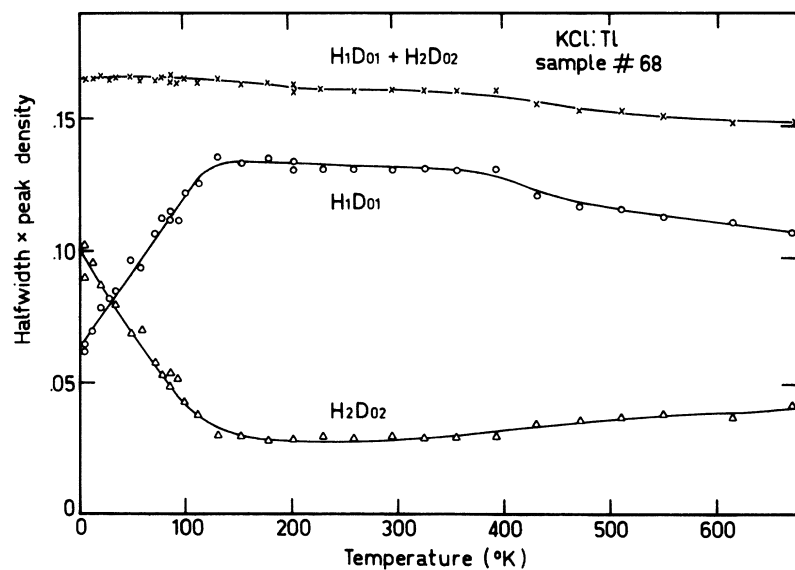


FIG. 8. Temperature dependence of the products  $H_1D_{01}$ ,  $H_2D_{02}$  (proportional to the areas under  $A_1$  and  $A_2$ , respectively), and of their sum.

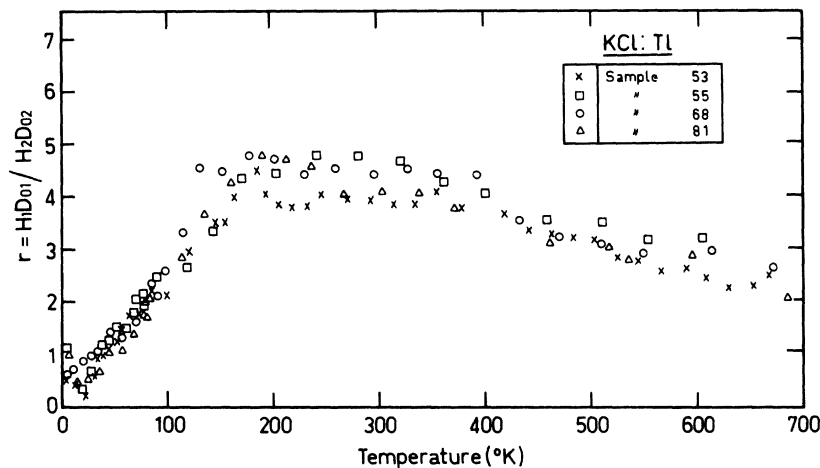


FIG. 9. Temperature dependence of the ratio of areas under  $A_1$  and  $A_2$  ( $r = H_1D_{01}/H_2D_{02}$ ) for different samples.

approximately also to the oscillator strength of the transition involved. Figure 8 shows, for sample 68, the dependence on temperature of  $H_1D_{01}$ ,  $H_2D_{02}$ , and of the sum  $H_1D_{01} + H_2D_{02}$ . The sum curve shows that the oscillator strength of the total  $A$  band drops very slowly with temperature (by about 10% on warming from 4 to nearly 700 °K).

The individual components do not behave as smoothly as the sum. The area under  $A_1$  grows towards a maximum near 150 °K, and  $H_2D_{02}$  decreases in the same temperature range, so that the ratio  $r = H_1D_{01}/H_2D_{02}$  reaches values of 4–5 (see Fig. 9). At higher temperatures  $H_1D_{01}$  decreases while  $H_2D_{02}$  tends to increase.

#### D. Comparison of Crystals with Different Tl Content

The structure of the  $A$  band was found to be the same in all the crystals examined in spite of their

different thallium content. This includes the parameters of the components, their relative intensities, and their temperature dependence. In the following we shall show a few examples for the almost identical behavior of the different samples. Figure 9 gives the ratio  $r = H_1D_{01}/H_2D_{02}$  as a function of temperature. Points for the four samples fall almost on a single curve. The value of  $r$  is less than 1 near 4 °K, rises to about 5 near 170 °K, and then falls back to about 2 at 700 °K.

To enable comparison of optical densities in crystals differing in thickness and thallium concentrations, we introduce the absorption cross section, or the absorption per ion per unit volume,  $\sigma(E)$ , given<sup>5</sup> by

$$\sigma(E) = (2.303/Nd)D(E) \\ = [(1.437 \times 10^{-22})/Cd]D(E) \text{ cm}^{-2}, \quad (3)$$

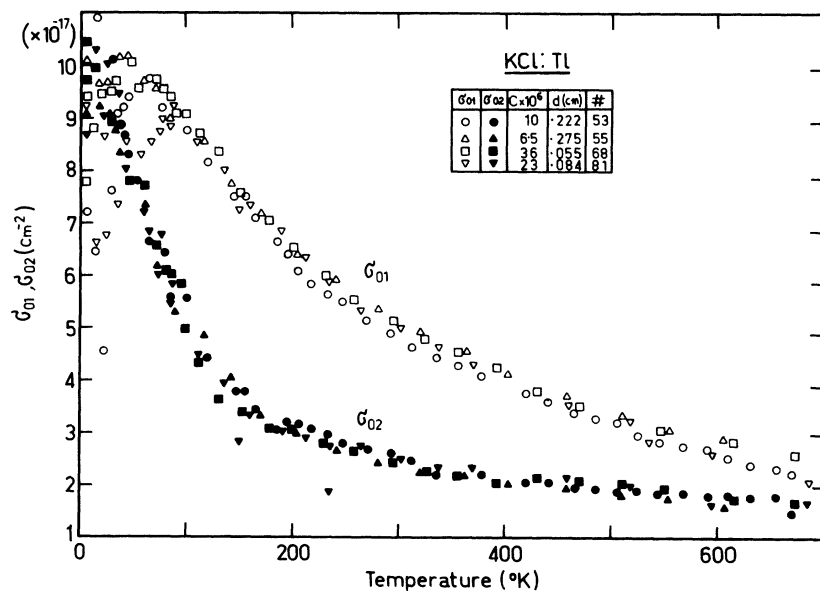


FIG. 10. Temperature dependence of the absorption cross section of the maxima of  $A_1$  and  $A_2$  ( $\sigma_{01}$  and  $\sigma_{02}$ ).

where  $N$  is the number of thallium ions per  $\text{cm}^3$ ,  $C$  is the molar fraction of thallium, and  $d$  is the thickness of the crystal in centimeters.  $\sigma(E)$  was shown by Wagner<sup>5</sup> to be independent of thallium concentration. Figure 10 describes the temperature dependence of the absorption cross sections at the maxima of  $A_1$  and  $A_2$  ( $\sigma_{01}$  and  $\sigma_{02}$ , respectively). Except for some scattering at low temperatures, the experimental points for all samples fall on just one pair of curves. This shows that not only the total  $A$  absorption, but also its resolution into components and their temperature dependence do not depend on the Tl concentration.

Figure 11 shows the temperature dependence of the half-widths for four samples. By the configuration coordinate approach the half-width should be given by

$$H = H_0 [\coth(\theta/T)]^{1/2}, \quad (4)$$

where  $H_0$  is the half-width, and  $\theta = \hbar\omega/2k$  is a characteristic temperature (with  $\hbar\omega$  the vibrational energy and  $k$  Boltzmann's constant). At high temperatures ( $T \gg \theta$ ), one obtains  $\theta \approx (H_0/H)^2 T$ , from which  $\theta$  can be estimated. Thus we obtained  $\theta_1 = 27^\circ\text{K}$ , and  $\theta_2 = 100^\circ\text{K}$  for  $A_1$  and  $A_2$ , respectively. These values were used in plotting the  $H_1$  and  $H_2$  curves in Fig. 11. The points for all samples fall on practically the same curves.  $H_1$  gives a straight line over almost the whole temperature range.  $H_2$ , on the other hand, does not fit a straight line; it deviates especially below  $200^\circ\text{K}$ , where it stays almost constant (see also Fig. 6). Figure 11 gives also the dependence of the separation  $\Delta E$  on temperature. All samples give nearly the same curve fitting a relation similar to Eq. (4) with  $\theta_2 = 100^\circ\text{K}$ .

## V. DISCUSSION

Esser and Levy<sup>6</sup> concluded that the  $A$  band in  $\text{KCl:Tl}$  has two components up to  $200^\circ\text{K}$ , and three at higher temperatures. Our results do not support this conclusion. Deviations of the  $A$  band from the sum of two Gaussians were generally within the experimental error of the measurements. The mean error curve (Fig. 4) with its minimum near  $170^\circ\text{K}$  may indicate that at other temperatures part of the deviation from the sum of two Gaussians could be real. The differences, however, being very small, do not justify the introduction of a third component. In addition, the two-step analysis (Fig. 5) giving only two Gaussians also supports this conclusion. The smaller mean errors in the three-Gaussian analysis may have resulted from the addition of the three more free parameters, which can be expected to reduce the error, especially when a systematic deviation enters. For example, the higher noise, scattering, and luminescence in the region of high optical densities near the peak of the band may increase the error

in density measurements. To check for the sensitivity of the three-Gaussian analysis to such errors, we submitted for analysis a curve composed of two pure Gaussians with small distortions (up to 0.03 density units) near the peak of one component. The analysis indeed gave three Gaussians (with a density of about 0.2 at the maximum of the smallest component, and a mean error of only  $1 \times 10^{-3}$ ). In contrast to this behavior, the two-Gaussian analysis was hardly affected by the introduced distortions.

It should be noted that, in spite of the differences, our results agree in many points with those obtained by Esser and Levy. There is almost full agreement in the parameters of  $A_2$  ( $A_3$  in Ref. 6) including the fact that the half-width of  $A_2$  remained almost constant up to nearly  $200^\circ\text{K}$ . There is also good agreement in the parameters of  $A_1$  up to  $200^\circ\text{K}$ .

The structure in the absorption bands of heavy ions in alkali halides has been attributed to the dynamical Jahn-Teller effect.<sup>13</sup> This approach has been treated theoretically by Kristofel,<sup>14</sup> who assumed the breakdown of the Condon approximation, and by Toyozawa and Inoue,<sup>15</sup> Cho,<sup>16</sup> and others, who relied on this approximation. The observed

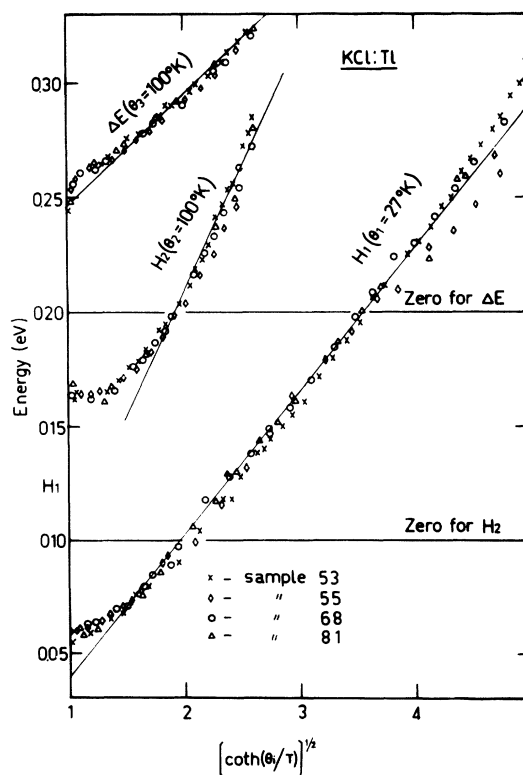


FIG. 11. Half-widths ( $H_1$  and  $H_2$ ) and separation ( $\Delta E$ ) of  $A_1$  and  $A_2$  as function of  $[\coth(\theta/T)]^{1/2}$ . (The zero line for  $H_2$  is displaced by 0.10 and that for  $\Delta E$  by 0.20 eV).



triplet structure of the C band,<sup>1,6</sup> and the increase with  $T^{1/2}$  of the separation between the components at high temperatures has been predicted by either of the above theories. The present work gave for the A band a separation fitting a law similar to Eq. (4), which was expected theoretically.<sup>13</sup> Theory in its present stage of development, however, did not predict pure Gaussians for the components of the A band. The good fit of the A band to the sum of two Gaussians should be taken into account in theoretical treatments of the structure.

Observations on the unresolved A band give the impression that on warming from 4 °K,  $A_2$  increases and overwhelms  $A_1$  above a given temperature. Such a reversal has been claimed to happen in the A band of heavy-metal ions in alkali halides,<sup>1</sup> and to follow theoretically from the dynamic Jahn-Teller effect.<sup>14,15</sup> The "reversal" appeared also in our measurements: At about 130–140 °K the A-band maximum jumped from the vicinity of  $A_1$  to that of  $A_2$  (compare curves *a* and *b* of Fig. 2). This, however, was not a real reversal of intensities. Figure 6 shows that  $D_{01}$  and  $H_1$  are larger than  $D_{02}$  and  $H_2$ , respectively, at all temperatures except those near 4 °K. The apparent reversal (which occurred at the same temperature in all our samples) was caused by the fact that  $A_2$  remained narrow (about 0.065 eV), while  $A_1$  broadened continuously in this temperature range. In addition, the separation  $\Delta E$  grows slowly with temperature ( $\theta_3 = 100$  °K), and so protrusion of  $A_2$  above the broad  $A_1$  component comes about. The peak position of  $A_2$  showed a slight shift to higher energies at low temperatures (Fig. 7). Such a "blue shift" has been observed previously in various heavy-ion doped alkali halides.<sup>1,6,17</sup>

By the semiclassical Franck-Condon approximation, the triplet structure in heavy-metal doped alkali halides has been explained as due to the splitting of the degenerate excited state  $T_{1u}$  by interaction with the  $T_{2g}$  lattice vibration.<sup>15,16</sup> The A band should, therefore, also have a triplet structure. To explain the observed doublet structure, Toyozawa and Inoue<sup>15</sup> assumed two components to coalesce into one band by the interaction between the A and B bands through the  $T_{2g}$  mode. This interaction should decrease with the increase in separation of the A and B bands. In KCl:Tl, this separation is quite large (nearly 1 eV), and so it is possible that the third component is not completely canceled. If this is the case, the small third component appearing at low temperatures in the three-Gaussian analysis (see curve *b* of Fig. 3) may indicate the remnescent third component predicted by Toyozawa and Inoue at low temperatures, when the quadratic interaction term becomes less effective (see Ref. 15, Fig. 11).

As already pointed out by Cho,<sup>14</sup> quantitatively there is still a disagreement between theory and experimental observations. Further observations on the splitting of the heavy-metal ion bands in crystals, both in absorption and emission, should lead to a refinement in the theory, and to a better agreement between theory and experimental observations.

#### ACKNOWLEDGMENTS

We acknowledge the help of I. Nathanson of our Crystals Growth Laboratory who grew the crystals used in the present work, and the help of S. Liberman in computer programming.

<sup>1</sup>A. Fukuda, *J. Phys. Soc. Japan* **27**, 96 (1969); *Sci. Light (Tokyo)* **13**, 64 (1964). The latter contains an extensive bibliography of earlier work on the subject.

<sup>2</sup>P. H. Yuster and C. J. Delbecq, *J. Chem. Phys.* **21**, 892 (1953).

<sup>3</sup>D. A. Patterson, *Phys. Rev.* **119**, 962 (1960).

<sup>4</sup>C. C. Klick, D. A. Patterson, and R. S. Knox, *Phys. Rev.* **133**, A1717 (1964).

<sup>5</sup>W. U. Wagner, *Z. Physik* **181**, 143 (1964).

<sup>6</sup>P. D. Esser and P. W. Levy, in *Proceedings of the International Symposium on Color Centers in Alkali Halides*, Rome, Italy, 1968, p. 87 (unpublished); *Bull. Am. Phys. Soc.* **14**, 325 (1969).

<sup>7</sup>F. Seitz, *J. Chem. Phys.* **6**, 150 (1938).

<sup>8</sup>F. E. Williams, *J. Chem. Phys.* **19**, 457 (1951).

<sup>9</sup>C. J. Delbecq, A. K. Ghosh, and P. H. Yuster, *Phys. Rev.* **151**, 599 (1966).

<sup>10</sup>(a) NONLINEAR LEAST SQUARES, Share Program Library No. 3094; (b) CREEP, Constrained NonLinear Estimation Package, Share Program Library No. 3492;

(c) BMDX85-BMD, Biomedical Computer Programs, x Series Supplement, edited by W. J. Dixon (University of California Press, Berkeley, Calif. 1969).

<sup>11</sup>In a few cases the exponent of  $E$  was also left as a free parameter. The computer gave for it values close to 4 (in the first attempt it gave the value 3.97!).

<sup>12</sup>A simple analysis shows that in most cases the overlap tends to give larger half-widths compared to the real ones (compare to half-widths given below).

<sup>13</sup>See review article by M. D. Sturge, in *Solid State Physics*, edited by F. Seitz and D. Turnbull (Academic, New York, 1967), Vol. 20, p. 199.

<sup>14</sup>N. N. Kristofel, *Opt. i Spektroskopiya* **22**, 74 (1966) [*Opt. Spectry. (USSR)* **22**, 36 (1967)].

<sup>15</sup>Y. Toyozawa and M. Inoue, *J. Phys. Soc. Japan* **21**, 1633 (1966).

<sup>16</sup>K. Cho, *J. Phys. Soc. Japan* **25**, 1372 (1968).

<sup>17</sup>T. Mabuchi, A. Fukuda, and R. Onaka, *Sci. Light (Tokyo)* **15**, 68 (1966).